Connected Vehicles Based Traffic Signal Timing Optimization

Wan Li, Xuegang (Jeff) Ban

This is the author's version of a work that has been published in IEEE Transactions on Intelligent Transportation Systems. The final version can be found here: 10.1109/IVS.2017.7995896

Connected Vehicles Based Traffic Signal Timing Optimization

Wan Li, Xuegang (Jeff) Ban*

***Abstract*— We study the traffic signal control problem with connected vehicles (CVs) by assuming a fixed cycle length so that the proposed model can be extended readily for the coordination of multiple signals. The problem can be first formulated as a mixed-integer nonlinear program, by considering information of individual vehicle's trajectories (i.e., second-by-second vehicle locations and speeds) and their realistic driving/car-following behaviors. The objective function is to minimize the weighted sum of total fuel consumption and travel time. Due to the large dimension of the problem and the complexity of the nonlinear car-following model, solving the nonlinear program directly is challenging. We then reformulate the problem as a Dynamic programming (DP) model by dividing the timing decisions into stages (one stage for a signal phase) and approximating the fuel consumption and travel time of a stage as functions of the state and decision variables of the stage. We also propose a two-step method to make sure that the obtained optimal solution can lead to the fixed cycle length. Numerical experiments are provided to test the performance of the proposed model using data generated by traffic simulation.**

***Index Terms*— Connected Vehicles, Traffic Signal Optimization, Mixed Integer Nonlinear Program, Dynamic Programming, End Stage Cost, Branch and Bound.**

I. Introduction

As a critical infrastructure that is crucial to the economy and the daily life of everyone, transportation also creates severe congestion and consumes tremendous energy. In the United States, e.g., the gasoline consumption by the transportation sector was about 143.37 billion gallons in 2016, a daily average of about 9.33 million barrels [1]. At the same time, traffic congestion on urban roads has caused extra fuel consumption as well as additional travel delays. The 2015 Urban Mobility Scorecard [2] estimated that U.S. highway congestion costs \$160 billion a year, and an average American commuter loses 42 hours per year due to traffic congestion. Therefore, it is imperative to reduce traffic delay and improve transportation energy efficiency in urban areas.

Fuel consumption and traffic delay in urban areas can be reduced by optimizing traffic signal control strategies. Traditional traffic signal control problems have been extensively investigated, with a variety of methods such as fixed-time control, actuated control, and adaptive control [3]. The adaptive signal control methods (aka the most advanced traffic signal control methods so far), e.g., include swarm algorithm [4], platoon-based algorithms [5], rolling horizon approaches [6], and oversaturation algorithm [7], among others. A comprehensive discussion of the signal control algorithms can be found in [8].

Urban traffic signal control can be further enhanced by the connected vehicle (CV) technology [9]. CV enables vehicle to vehicle (V2V) and vehicle to infrastructure (V2I) communications through dedicated short-range communications (DSRC) and other means. With the V2V communications, location and speed information can be exchanged among nearby vehicles. With the V2I communications, vehicles can communicate with traffic signals, work zones, tollbooths, and other types of infrastructure to exchange information such as vehicle trajectories, traffic conditions, and signal timing. Such data/information exchange among vehicles and between vehicles and infrastructure has the potential to significantly improve traffic mobility and fuel consumption efficiency at signalized intersections.

There have been various traffic signal control studies under the CV environment. Goodall et al [10] developed the predictive microscopic simulation algorithm (PMSA) to control traffic signal. The strategy can minimize total delays, or the combination of delays, stops, and decelerations over a 15-second time period by considering instantaneous vehicle data. The study showed that at low or mid-level traffic volume, their proposed algorithm outperformed state-of-the-practice coordinated-actuated timing plan, while the performance got worse during saturated and oversaturated conditions. He et al. [11] developed the platoon-based arterial multi-modal signal control with online data (PAMSCOD) algorithm, with signal updated every 30 seconds. A mixed-integer nonlinear program (MINLP) was solved to determine future optimal signal plan. Simulation results in VISSIM showed that delays were significantly reduced under both non-saturated and oversaturated traffic conditions compared to traditional state-of-the-practice coordinated actuated signal control. Lee and Park [12] developed a cumulative travel-time responsive (CTR) real-time intersection control algorithm in the CV environment. They examined the different penetration rates of CV and level of congestion. Kalman filtering technique was utilized to estimate the cumulative of travel time under various penetration rates. Among various types of methods, dynamic programming (DP) is one of the most commonly used technique to solve the discretized signal control problems. It was first applied in Sen and Head [13] to optimize traffic signal timing. The idea was later applied in Chen et al. [14] and Feng et al.[15]. In particular, Feng et al. [15] proposed a bi-level formulation for optimizing

The authors are with Department of Civil and Environmental Engineering, University of Washington, Seattle, WA, 98195. E-mail: wan5@uw.edu, banx@uw.edu

signal timing of a single intersection: the upper level is to optimize for the barrier lengths and the lower level is to optimize for the phase times. However, most of these studies assumed varying cycle lengths, which may not be readily applied to multiple intersections if signal coordination is needed. There are a few exceptions. He et al. [11] and Zamanipour et al. [16] incorporated fixed cycle length (thus coordination) as a virtual priority request, which introduces additional constraints in MILP. Beak et al. [17] extended Feng et al. [15] to impose the fixed cycle length, albeit with a bi-level formulation. First, they imposed extra constraints to the upper level to ensure a fixed cycle length. The revised intersection-level model (with a fixed cycle length) is then integrated into a corridor-level model for signal coordination. In this paper, we develop a two-step method to consider fixed cycle length at the intersection level. This avoids the use of the bi-level structure in Feng et al. [15] and Beak et al. [17], which is computationally more efficient.

Fuel consumption is a major consideration that researchers have been trying to evaluate when they develop traffic signal strategies. Zhao et al. [18] proposed a signal timing optimization strategy to minimize the combined total energy consumption and traffic delay, considering the fuel consumption of individual vehicles. Vehicles' trajectories were predicted second by second using the Nagel-Schreckenber model. An iterative grid search algorithm was used to solve the optimized signal timing. The method however ignored left-turn traffic and cannot be applied to real-world intersections. More studies that considered fuel prediction models can be found in [19]-[22]. Here we do not assume vehicles are autonomously driving, and therefore intersection control strategies, such as those based on reservation [23]-[26] and other methods [27]-[29], will not be discussed.

This study aims to optimize signal timing in the CV environment considering individual vehicle's trajectories. As discussed above, most existing signal optimization methods work for single intersections and assume variable cycle lengths, with a few exceptions [16][17][30]-[32]. Coordination occurs when two or more traffic signals are working together so that moving vehicles could go through the intersections with minimum delays and the least number of stops. The cycle lengths of coordinated traffic signals are often fixed as a constant. In this study, we focus on a single intersection and assume a fixed cycle length such that the proposed method can be readily extended in the future to coordinate multiple signals in a traffic corridor or network. *First*, we formulate the CV-based signal control problem as a MINLP, by considering information of *individual* vehicle's trajectories (i.e., second-by-second vehicle locations and speeds) and their realistic driving/car-following behavior, captured by the Intelligent Driving Model (IDM). The objective function is to minimize the weighted sum of total system fuel consumption and travel time. Due to the large dimension of the problem and the complexity of the nonlinear car-following model, solving the nonlinear program directly can be challenging. *Secondly*, we reformulate the problem as a DP model by dividing the timing decisions into stages (one stage for a signal phase) and approximating the total fuel consumption and travel time of a stage as functions of the state and decision variables. We note that imposing the fixed cycle length constraint will invalidate the DP formulation. We then apply a two-step method to resolve this issue. The first step is to add an end-stage cost to the DP formulation. The cost measures how much the DP solution violates the fixed cycle length constraint. This step forces the DP to produce a solution with a cycle length that is close enough to the given fixed cycle length. The second step is a branch and bound method to further refine the DP solution to obtain a solution of the original problem, with the exact fixed cycle length. Numerical experiments are provided in the paper to test the performance of the proposed model using data generated by traffic simulation.

The main contributions of the paper include:

1. This study accounts for the *individual* vehicle's trajectories (i.e., second-by-second vehicle locations and speeds) into signal timing optimization, which can be provided by CV technologies.
2. A signal optimization strategy is developed for a single intersection with *fixed cycle length*, which can be easily extended for signal coordination. It is formulated as a mixed-integer nonlinear program (MINLP). The *MINLP* model may have a large dimension and is hard to solve.
3. A *DP* reformulation is proposed via certain approximation schemes. To ensure the fixed cycle length, a *two-step method* is developed: adding the end-stage cost and a branch and bound algorithm.

II. Formulating Signal Control as a Mixed-Integer Nonlinear Program

In this section, the signal control problem with the fixed cycle length constraint is formulated as a MINLP. Here we adopt the dual-ring method for signal design as it can properly balance safety and efficiency of traffic signal control [3][15]. This is important since the primary objective of traffic signal control is to ensure safety, i.e., to minimize conflicts [3], while mobility is also important as long as safety is ensured. The signal configuration in a dual-ring diagram is shown in Figure 1. Without loss of generality, we assume the eastbound/ westbound (EB/WB) through movements (2 and 6 in Figure 1) are the major movements and thus cannot be skipped (i.e., for coordination purposes). Other phases may be skipped by setting the corresponding phase durations as zero. We also assume a cycle always starts with movements 2 and 6. Such a signal timing plan can be considered as 6 *groups* with a sequence of 8 *phases* in Figure 2. Noted that phase 2 and 3 in group 2 cannot be realized at the same time, indicating that at least one of the two phases need to be skipped. Same situation happens for phase 6 and 7 in group 5. In this paper, the continuous time is discretized into 1s intervals.

Based on the literature [33], the maximum/minimum green parameters are defined for a movement. In this paper, we define maximum/minimum green based on phases, which is consistent to [33] and Sen and Head [13] when phase overlaps are not allowed, i.e., only phase 1, 4, 5, and 8 exist, as shown in Figure 2. A phase overlap refers to a pair of phases that contain one common movement, e.g., phase 1 contains movement 2 and 6, and phase 2 contains movement 2 and 5, occurring in sequence would allow movement 2 to "overlap". If phase overlaps exist, minimum greens for the overlap phases (phase 2, 3, 6, and 7) are set to be zero in order to allow them to be skipped, the minimum greens for phases 1,4,5,8 remain the same. Maximum greens for the overlap phases (2, 3, 6, and 7) are set to be a small value, e.g., 10s, while maximum green for the non-overlap phases need to be deducted by a corresponding value, e.g., the maximum green for phase 1 needs to subtract 10s. In the numerical test, we set the maximum green for non-overlap phases (1, 4, 5, and 8) as the cycle length, minimum green for non-overlap phases as 5s. For overlap phases (2, 3, 6, 7), the maximum green is half of the cycle length and minimum green is zero. This is designed to allow DP to search for sufficiently large state spaces to find an optimal solution, with a reasonable computational effort. The numerical tests suggest that selecting different values as maximum/minimum greens does not have significant influence on the total cost.

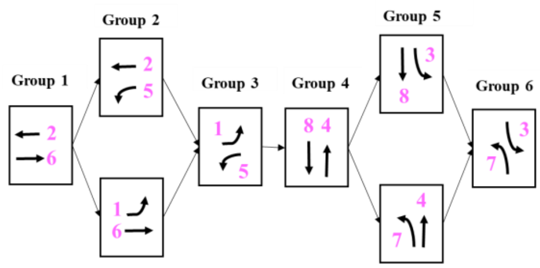

Figure 1 Traffic signal configuration [35]

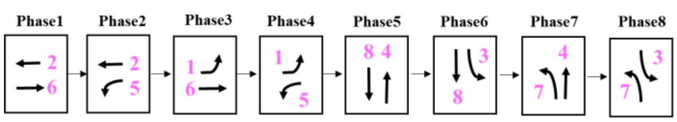

Figure 2 Traffic signal configuration

Parameters

C	Cycle length (s).
m_F	Monetary value of fuel (\$/gal), e.g., \$3/gal.
m_{TT}	Monetary value of travel time (\$/s). e.g., \$12/h (\$0.005/s).
e	Idle fuel consumption rate (gal/h).
l_n	Length of vehicle n (m).
δ	Acceleration exponent in IDM. It usually set at 4.
H	Desired time headway (s), e.g., 1.5s.
a_{max}	Maximum acceleration rate ($\mathrm{m/s^2}$), e.g., 1 $\mathrm{m/s^2}$.
b_{max}	Maximum deceleration rate ($\mathrm{m/s^2}$), e.g., 3 $\mathrm{m/s^2}$.
s_{on}	Gap between vehicles in complete standstill traffic jams (m), e.g., 2m.
v_0	Vehicle desired speed (m/s).
g_k^{min}	Minimum effective green time of phase k (s).
g_k^{max}	Maximum effective green time of phase k (s).
k	Signal phase, k = 1, 2… 8.
$\bar{d}_n^0, \bar{d}_n^1$	Entrance location and exit location of the incoming approach of vehicle n (m).
$d_{signal,n}$	The location of the nearest front signal of vehicle n (m).

Variables

$FC_{n,t}$	Fuel consumption for vehicle n at time t (gal/s).
$TT_{n,t}$	Travel time of vehicle n at time t (s).
$FC_{I,n}$	Fuel consumption for vehicle n at the idle status (gal/s).
$FC_{s,n,t}$	Fuel consumption of vehicle n at time t at the moving status (gal/meter).
g_k^i	Effective green time allocated to phase k of cycle i (s).
$v_{n,t}$	Speed of vehicle n at time t (m/s).
$d_{n,t}$	Location of vehicle n at time t (m).
$I_{n,t}$	Idle status indicator for vehicle n at time t.
$S_{k,t}$	Traffic signal status of phase group k at time t.
$\bar{k}$	Current phase index at time t. It represents the phase that is currently given the green light.
$Z_{n,t}$	Traffic signal status for vehicle n at time t.
$Y_{n,t}$	Traffic signal indicator. It takes 1 if the preceding vehicle is traffic signal.
$s_{n,t}$	Vehicle gap (m).
$\Delta v_{n,t}$	Speed difference between vehicle n and $n-1$ at time t (m/s).
$a_{n,t}$	Acceleration rate for vehicle n at time t ($\mathrm{m/s^2}$).
$y_{t,1}, y_{t,2}, y_{t,3}, y_{t,4}$ $y_{n,t,1}, y_{n,t,2}$	Binary variables (auxiliary).

The objective of the CV-based signal optimization problem can be formulated as minimizing the weighted sum of total fuel consumption and travel time [18][34] of all vehicles approaching the intersection:

$$min\, F = \sum_{t=1}^{T}\sum_{n=1}^{N}\left(m_F FC_{n,t} + m_{TT} TT_{n,t}\right) \tag{1}$$

$FC_{n,t}$ and $TT_{n,t}$ are the fuel consumption and travel time for vehicle n at time t. The corresponding parameters m_F and m_{TT} are the "value of fuel" and "value of time" respectively. Eq. (1) indicates that the objective function here considers the travel time and fuel consumption for all vehicles in the network for total time span T. N here is the total number of vehicles. Eq. (2) calculates the fuel consumption of vehicle n at time t, which is determined by the vehicle status. If vehicle n is idling at time t, the indicator variable for idle status, $I_n(t)$, takes one and the fuel consumption model $FC_{I,n}$ is applied, as shown in Eq. (4). Otherwise, $I_n(t)$ tales zero and Eq. (5) will be applied, which calculates the fuel consumption of vehicle n at the moving status. The threshold value for idle status is 2.2 m/s (5mph), which is provided in Zhao et al [18]. Eq. (3b) reformulate (3a) using the "big M" method [36] by establishing a relationship between speed $v_{n,t}$ and idle status indicator $I_{n,t}$. M here is a large number and M=1,000 is used in this paper. The model could be used to calculate fuel consumption for different vehicle types, including sedan, SUV, bus, EV, and Hybrid Electric (HEV). Zhao et al [18] provided the calibrated parameters in Eq. (4) and (5) for different vehicle types, as shown in Table 1.

$$FC_{n,t} = FC_{s,n,t} * v_{n,t} * \left(1 - I_{n,t}\right) + FC_{I,n} * I_{n,t} \tag{2}$$

$$I_{n,t} = \begin{cases} 1, & if\ v_{n,t} < 2.2, \quad idling\ at\ time\ t \\ 0, & if\ v_{n,t} \geq 2.2, moving\ at\ time\ t \end{cases} \tag{3a}$$

$$\begin{cases} v_{n,t} - 2.2 < (1 - I_{n,t})M \\ v_{n,t} - 2.2 + I_{n,t}\mathrm{M} \geq 0 \end{cases} \tag{3b}$$

$$FC_{I,n} = e \tag{4}$$

$$FC_{s,n,t} = \frac{a}{v_{n,t}} + b + cv_{n,t} + dv_{n,t}^2 \tag{5}$$

Table 1 Parameter identification for fuel consumption models

Vehicle Type	Parameters				
	a	*b*	*c*	*d*	*e*
1 EV	4.74e-2	2.66e-3	6.37e-5	1.49e-6	0
2 HEV (SOC0=0.7)	1.83e-1	3.67e-3	1.27e-4	2.39e-6	0
3 HEV (SOC0=0.6)	1.83e-1	3.67e-3	1.27e-4	2.39e-6	0
4 HEV (SOC0=0.5)	1.82e-1	1.51e-3	5.67e-4	-4.35e-6	0
5 Sedan	4.75e-1	-8.50e-3	5.41e-4	1.04e-7	0.211
6 SUV	7.44e-1	-1.23e-2	6.78e-4	5.29e-6	0.491
7 Bus	2.51e+0	3.03e-2	4.18e-3	-1.26e-5	1.184

As aforementioned, this study assumes the cycle length be fixed for the whole time span *T* (e.g., a few hours). The effective green time for each phase *k* of cycle *i*, g_k^i, must sum up to the (fixed) cycle length *C*, as shown in Eq. (6). We assume there is no transition time between phases. There are eight phases in Figure 1 so K = 8. Eq. (7) indicates the bounds of the green time g_k^i. For phases that can be skipped, $g_k^{min} = 0$. Eq. (8-9) indicate phase 2 and 3 (and phase 6 and phase 7) cannot be realized for the same cycle *i*. At least one of the two variables, e.g., g_2^i (g_6^i) and g_3^i (g_7^i)), needs to be zero.

$$\sum_{k=1}^{K} g_k^i = C \qquad \forall\, i \in 1,2,\ldots I \tag{6}$$

$$g_k^{min} \le g_k^i \le g_k^{max} \tag{7}$$

$$g_2^i * g_3^i = 0 \tag{8}$$

$$g_6^i * g_7^i = 0 \tag{9}$$

Each intersection contains multiple movements with two movements served by a phase k. Variable $S_{k,t}$ denotes the signal status at time t for phase *k*, as shown in Eq. (10a). Noted that when k =0, $g_k^i = 0$. It takes one if the signal status at the current time stamp is red and zero if it is green. The variable $\bar{k}$ is the current phase index at time *t* (i.e., 1, 2… 8). It represents the phase in Figure 1 that is currently given the green light. Eq. (10b) reformulates (10a) using two binary variables $y_{t,1}$ and $y_{t,2}$ based on the big *M* concept.

$$S_{k,t} = \begin{cases} 0, \ if \ \sum_{k=0}^{\bar{k}-1} g_k^i \le (t \ mod \ C) < \sum_{k=0}^{\bar{k}} g_k^i \\ 1, \qquad\qquad\qquad\qquad\qquad otherwise \end{cases} \tag{10a}$$

$$\begin{cases} \sum_{k=0}^{\bar{k}} g_k^i - (t \ mod \ C) + y_{t,1}M > 0 \\ \sum_{k=0}^{\bar{k}} g_k^i - (t \ mod \ C) \le (1 - y_{t,1})M \\ (t \ mod \ C) - \sum_{k=0}^{\bar{k}-1} g_k^i + y_{t,2}M \ge 0 \\ (t \ mod \ C) - \sum_{k=0}^{\bar{k}-1} g_k^i < (1 - y_{t,2})M \\ S_{k,t} = y_{t,1} + y_{t,2} \end{cases} \tag{10b}$$

Eq. (11) use indicator variables $y_{t,3}$ and $y_{t,4}$ together to identify whether vehicle *n* is within the "range" of the incoming approach defined by $\bar{d}_n^0$ and $\bar{d}_n^1$. Both of them will be zero if vehicle *n* is within the range; otherwise, one of the will be 1. Furthermore, the signal status $Z_{n,t}$ at time *t* for vehicle *n* could be determined as long as the incoming approach of vehicle *n* is identified. There are usually two phases that may serve vehicle *n*, e.g., both phase 1 and phase 2 could serve vehicle *n* if it comes from movement 2. In this case, we first define $\bar{Z}_{n,t}$, the "minimum" signal status of the two phases that serve vehicle *n*; see equation (12a) below. This is to ensure that as long as one of the two phases is green ($S_{k,t}$ is zero), vehicle *n* will see green ($\bar{Z}_{n,t}$ is zero). Note that signal status $Z_{n,t}$ and $S_{k,t}$ are different. Before the vehicle enters the intersection range, the trajectory of the vehicle should not be impacted by the signal. This is guaranteed by Eq. (12b) that $Z_{n,t}$ is always zero (green) before the vehicle enters the intersection range so that neither the location nor the speed of the vehicle is impacted by $Z_{n,t}$; see equations (14) and (15). Once the vehicle enters the range, $Z_{n,t}$ is the same as $\bar{Z}_{n,t}$ as shown by equations (11) and (12b), which also equals to one of the $S_{k,t}$'s as shown in (12a).

$$\begin{cases} d_{n,t} - \bar{d}_n^1 \le y_{t,3}M \\ d_{n,t} - \bar{d}_{n,}^1 + (1 - y_{t,3})M \ge 0 \\ d_{n,t} - \bar{d}_n^0 + y_{t,4}M \ge 0 \\ d_{n,t} - \bar{d}_n^0 \le (1 - y_{t,4})M \end{cases} \tag{11}$$

$\bar{Z}_{n,t} = min\{S_{k,t}\}$ for all phase *k* that may serve vehicle *n* (12a)

$$Z_{n,t} = \bar{Z}_{n,t} - \frac{\bar{Z}_{n,t} + (y_{t,3} + y_{t,4}) - |\bar{Z}_{n,t} - (y_{t,3} + y_{t,4})|}{2} \tag{12b}$$

The CV-based signal timing strategies in this paper require information on real time vehicle trajectories. This study assumes the 100% penetration rate of CVs. Vehicle trajectories can be transmitted when a vehicle enters the boundary of an intersection. Furthermore, to optimize signal timing for the current and future cycles, future vehicle trajectories are needed. For this, the Intelligent Driver Model (IDM) [37] is applied to simulate vehicle trajectories. IDM is a car-following model that fits better with CV [38]. We assume that there is only one lane (and a dedicated left turn lane at the intersection) per incoming approach, so there is no lane changing behavior involved. It is necessary to account for the signal status in the prediction of traffic flow propagation when applying IDM. For this, we model the red signal as a "standing vehicle" with speed equal to zero. It would disappear if the signal turns green. Eq. (13a) indicates whether the front object of vehicle *n* is a real vehicle or a standing vehicle (traffic signal) by comparing the relative location of the front vehicle $n-1$, vehicle n, and the nearest traffic signal in front of vehicle *n*. The binary variable $Y_{n,t}$ takes one if the front "vehicle" is the traffic signal (could be red or green) at location $d_{signal,n}$ with speed zero. If $y_{n,t}$ is zero, the front vehicle $n-1$ is a real vehicle with location $d_{n-1,t}$ and speed $v_{n-1,t}$. This helps update the vehicle trajectories in IDM as shown later. Eq. (13b) reformulate (13a) using the big *M* method and two binary variables $y_{n,t,1}$ and $y_{n,t,2}$.

$$Y_{n,t} = \begin{cases} 1, if \ x_{n,t} < d_{signal,n} < x_{n-1,t} \\ 0, \qquad\qquad\qquad\qquad otherwise \end{cases} \tag{13a}$$

$$\begin{cases} d_{signal,n} - d_{n-1,t} < y_{n,t,1}M \\ d_{signal,n} - d_{n-1,t} + (1 - y_{n,t,1})M \ge 0 \\ d_{n,t} - d_{signal,n} < y_{n,t,2}M \\ d_{n,t} - d_{signal,n} + (1 - y_{n,t,2})M \ge 0 \\ Y_{n,t} = 1 - (y_{n,t,1} + y_{n,t,2}) \end{cases} \tag{13b}$$

Using IDM, Eq. (14-15) identify the vehicle location and speed of the preceding "vehicle" $n-1$, which could be a real vehicle or the nearest front signal.

$$f_{n-1,t}^d = d_{n-1,t} * [1 - \frac{Y_{n,t} + Z_{n,t} - |Y_{n,t} - Z_{n,t}|}{2}] + d_{signal,n,t} * \frac{Y_{n,t} + Z_{n,t} - |Y_{n,t} - Z_{n,t}|}{2} \tag{14}$$

$$f_{n-1,t}^v = v_{n-1,t} * [1 - \frac{Y_{n,t} + Z_{n,t} - |Y_{n,t} - Z_{n,t}|}{2}] \tag{15}$$

Eq. (16-19) shows how IDM estimates the acceleration rate for vehicle n at each time interval, given the location and speed of vehicle $n-1$.

$$s_{n,t} = f^{d}_{n-1,t} - d_{n,t} - l_{n-1} \tag{16}$$

$$\Delta v_{n,t} = f^{v}_{n-1,t} - v_{n,t} \tag{17}$$

$$a_{n,t} = a_{max}[1 - \left(\frac{v_{n,t}}{v_0}\right)^{\delta} - \left(\frac{s^*(v_{n,t}), \Delta v_{n,t}}{s_{n,t}}\right)^2] \tag{18}$$

$$s^*(v_{n,t}, d_{n,t}) = s_{on} + v_{n,t}H + \frac{v_{n,t}\Delta v_{n,t}}{2\sqrt{a_{max}b_{max}}} \tag{19}$$

Eq. (20-21) are applied to update the trajectories for vehicle n at the next time interval $t+1$. More details of Eq. (14-21) can be found in [37]. In this paper, the values of the parameters in IDM are chosen as a = 1m/s^2, b =3 m/s^2, s_{on}= 2m, H = 1.5s, and δ = 4, according to [39].

$$v_{n,t+1} = max(0, v_{n,t} + a_{n,t}) \tag{20}$$

$$d_{n,t+1} = d_{n,t} + \frac{v_{n,t}+v_{n,t+1}}{2} \tag{21}$$

Eq. (1) – (21) is a MINLP for the CV-based signal control problem. It clearly shows that when individual vehicle status is considered for signal control, e.g., under the CV environment, the problem can be formulated as a very complex MINLP. This is mainly due to the different status of vehicles and signal phases, as well as the various if-then-else types of conditions (e.g., equations (3), (8), (13), and others) inherent to this coupled signal-vehicle optimization problem. In addition, since the variables of the model include the location and speed of each vehicle at each time interval, the dimension of the problem can be quite large. Furthermore, the IDM-based car following model is also very complex. Thus solving the model directly is quite challenging, and more tractable and efficient methods are needed. We next present one of such methods based on DP.

III. Dynamic Programming Formulation

DP provides a general framework to divide an optimization problem into multiple stages (under certain conditions), which could be solved sequentially one stage at a time. Here we divide the signal timing decisions into stages, one stage for a phase. We then approximate the total fuel consumption and travel time of a stage as functions of the state and decision variables of that stage only. The notation for DP is first summarized as follows; the unit of each variable/parameter is provided in parentheses

x_p	Decision variable, phase duration of stage p (s).
s_p	State variable, total time from beginning of the cycle to the end of stage p (s).
$X_p(s_p)$	The set of feasible control variable given stage variable s_p at stage p (s).
$V_p(s_p)$	Value function, the cumulative value of objective function from stage 1 up to stage p ($).
x_p^{min}	Minimum value of the decision variable at stage p (s).
x_p^{max}	Maximum value of the decision variable at stage p (s).
$f_p(s_p, x_p)$	Total cost at stage p, given state variable s_p, and decision variable x_p ($).
N_p	Total number of vehicles in phase p (veh).
$FC_{n,t}(s_p, x_p)$	Fuel consumption of the vehicle n at time t given stage variable s_p and decision variable x_p (gal/s).
$TT_{n,t}(s_p, x_p)$	Travel time of vehicle n at time t given stage variable s_p and decision variable x_p (s).
$FC_{s,n,t}(s_p, x_p)$	Fuel consumption of vehicle n at moving status at time t given stage variable s_p and decision variable x_p (gal/meter).
$FC_{I,n}(s_p, x_p)$	Fuel consumption of vehicle n at idle status at time t given stage variable s_p and decision variable x_p(gal/s).
$A_p(s_{p-1}, s_p)$	The number of arriving vehicles in the time interval $[s_{p-1}, s_p]$.
$M_p(x_p)$	The maximum number of vehicle that can be discharged during phase duration x_p.
$v_{n,t}(s_p, x_p)$	Approximated speed of vehicle n at time t given the stage variable s_p and decision variable x_p (m/s).
t_a	Arrival time at the predefined intersection boundary (distance L upstream of intersection) (s).
t_d	Time when vehicle joins the queue (started to slow down) (s).
t_0	Time when the vehicle fully stops (s).
t_{ac}	Time when vehicle starts to be discharged (s).
t_l	Time when the vehicle achieves the free flow speed v_0(s).
l_d	Distance upstream of end of queue or the stop line (if no queue) (m), e.g., 100m.
$V_p(s_p)$	Value function at phase p given state variable s_p.
σ	Tolerance of the fixed cycle length (s), e.g., 5s.

As shown in Figure 1 and Figure 2, there are eight stages in total. The state variable s_p is defined as the total number of time intervals from the beginning of the cycle to the end of stage p, while the decision variable x_p is the phase duration. Eq. (22-23) illustrate the relationship between state variable and decision variable. Parameter r denotes the effective clearance interval; see Sen and Head [13] for more details.

$$s_p = s_{p-1} + h(x_p) \tag{22}$$

$$h(x_p) = \begin{cases} 0, & if\ x_p = 0 \\ x_p + r, & other\ wise \end{cases} \tag{23}$$

Given the state variable s_p, the feasible set of decision variables could be determined based on Eq. (24):

$$X_p(s_p) = \begin{cases} 0, & if s_p < x^{min} \\ \{0, x_p^{min}, x_p^{min}+1, \dots, (\min(x_p^{max}, s_p)\}, & otherwise \end{cases} \tag{24}$$

To formulate the DP, we first assign the initial value function $V_0 = 0$. The DP starts from stage (phase) p = 1, and proceed recursively to p = 2, 3 … 8. At each stage, the method calculates the optimal decision variable $x_p^*(s_p)$ by minimizing the value function for each possible value of the state variable s_p in the forward recursion. Note that after stage 1, phase 2 or phase 3 may be chosen for the optimal decision variable, but not both; the same rule applies to phase 6 and phase 7. After the decision variables are estimated for all stages, the optimal decision of each stage can be retrieved in the backward recursion. The DP calculation process can be equivalently represented by an acyclic graph, as shown in Figure 3.

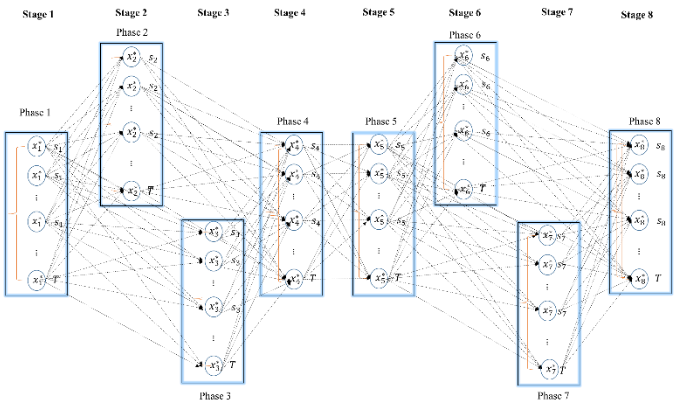

Figure 3 Acyclic graph of DP calculation process

However, in order to reformulate the signal control problem (1) – (21) as a DP, a critical condition is that the objective function in (1) can be expressed as the summation of the objective function of each stage. Furthermore, the stage-specific objective function (i.e., the sum of the vehicle fuel consumption and travel time of all vehicles in the stage) can be expressed as a function of the state and decision variables of that stage only [13]. This however is not true in general for most of the objectives we consider here, i.e., travel time or fuel consumption. It is especially so when we consider the data/information of individual vehicles (such as trajectories, speeds, delays, etc.). In the next subsection, we approximate the objective function of each stage so that it can be expressed as a function of the state and decision variables of the stage.

A. *Objective Function Approximation*

Eq. (25a) expresses the total fuel consumption and travel time of all the vehicles for phase p (i.e., it is from time s_{p-1} to s_p), where N_p is the total number of vehicles in phase p. In this paper, travel time of a vehicle is estimated by the summation of free flow travel time of the vehicle and the delay it encountered. As shown previously [13], the total delay (and thus travel time) of a stage in (25b) can be approximated as a function of the state and decision variables. We show in this subsection how the fuel consumption can be approximated as a function of the state and decision variables. As shown in (5) and rewritten in (26), fuel consumption is a function of vehicle speeds. Thus we aim to approximate the vehicle speed as a function of the state and decision variables.

$$Min \sum_{n=1}^{N_p} \sum_{s_{p-1}}^{s_p} f_p(s_p, x_p) \quad (25a)$$

$$f_p(s_p, x_p) \triangleq m_F FC_{n,t}(s_p, x_p) + m_t TT_{n,t}(s_p, x_p) \quad (25b)$$

$$FC_{n,t}(s_p, x_p) = FC_{s,n,t}(s_p, x_p) * v_{n,t}(s_p, x_p) * (1 - I_{n,t}) + FC_{I,n} * I_{n,t} \quad (26)$$

The speed of a vehicle is estimated based on the queue discharging process. Let $A_p(s_{p-1}, s_p)$ denote the number of arriving vehicles for phase p, i.e., during the time interval $[s_{p-1}, s_p]$. $M_p(x_p)$ denotes the maximum number of vehicle that can be discharged during the time interval of green time x_p.

As shown in [13], A_p and M_p can be expressed as functions of the state and decision variables of stage p only. We next show how the *speed* of a vehicle can be approximated as those variables. There are four possible cases for the speed of a vehicle arriving in stage p, as shown in Figure 4.

(1) Vehicle arrives during green signal at stage p and can pass freely through intersection.

$$\bar{v} = v_o \quad (27)$$

(2) Vehicle arrives during green at stage p but a queue already exists. The queue includes vehicles that were not discharged in the previous stage p-1 and the newly arrived vehicles at stage p before the current vehicle. Denote t_a the time when the current vehicle arrives at the predefined intersection boundary (distance l upstream of intersection), t_d the time when the vehicle joins the queue (started to slow down), t_0 the time when the vehicle fully stops, t_{ac} the time when the vehicle starts to be discharged, and t_l the time when the vehicle achieves the free flow speed v_0 again after being discharged. We assume the vehicle starts to decelerate with a constant rate at time t_d if queue exists. We can then approximate the average speed between t_d and t_0 as $\frac{v_0}{2}$. The same assumption applies to the acceleration process from t_{ac} to t_l. When the vehicle starts to decelerate at t_d, the distance between the vehicle and the stop line is denoted as l_d.

If the vehicle could pass the intersection within the current phase p (trajectory ① in Figure 4(b)), speed could be approximated using Eq. (28), otherwise (trajectory ②), vehicle has to wait until the next phase. In this case, we only apply first three conditions in Eq. (28) since $t_1 \geq s_p$. We could consider ② as a special case of ①.

$$v_{n,t}(s_p, x_p) = \begin{cases} v_0, & if\ t_a \leq t \leq t_d \\ \frac{v_0}{2}, & if\ t_d < t \leq t_0 \\ 0, & if\ t_0 < t \leq t_{ac} \\ \frac{v_0}{2}, & if\ t_{ac} < t \leq t_l \\ v_0, & if\ t_l < t \leq s_p \end{cases} \quad (28)$$

(3) Vehicle arrives during red signal at stage p. Figure 4 (c) and (d) are differentiated by whether queue exists at the end of stage p. If there is no queue, vehicle n will start to leave at $t_1(t_1 = s_p)$, otherwise it will have to wait for the queue to dissipate ($t_1 \geq s_p$). Here we only care about the vehicle status from time s_{p-1} to s_p. The speed of vehicle n arriving during red can be summarized as:

$$v_{n,t}(s_p, x_p) = \begin{cases} v_0, & if\ t_a \leq t \leq t_d \\ \frac{v_0}{2}, & if\ t_d < t \leq t_0 \\ 0, & if\ t_0 < t \leq s_p \end{cases} \quad (29)$$

After approximating the vehicle speed $\boldsymbol{v_{n,t}(s_p, x_p)}$ in the objective function for stage p based on the above four cases, the objective function can be approximated as a function of s_p and x_p only, as shown below:

$$V_p(s_p) = \min\{f_p(s_p, x_p) + V_{p-1}(s_{p-1}) | x_p \in X_p(s_p), p \in P\} \quad (30)$$

This means that Eq. (25), and the objective function of the MINLP in Section II as well, can be expressed as a function of $\boldsymbol{s_p}$ and $\boldsymbol{x_p}$ (for all p) only. Thus the problem can be reformulated as a DP. Detailed proof is straightforward and omitted here. Furthermore, after obtaining the optimal decision variable $\boldsymbol{x}_{\boldsymbol{p}}^{*}$ at stage p, IDM is applied to update the trajectories of all the vehicles from $\boldsymbol{s}_{\boldsymbol{p-1}}$ to $\boldsymbol{s}_{\boldsymbol{p}} = \boldsymbol{s}_{\boldsymbol{p-1}} + \boldsymbol{x}_{\boldsymbol{p}}^{*}$.

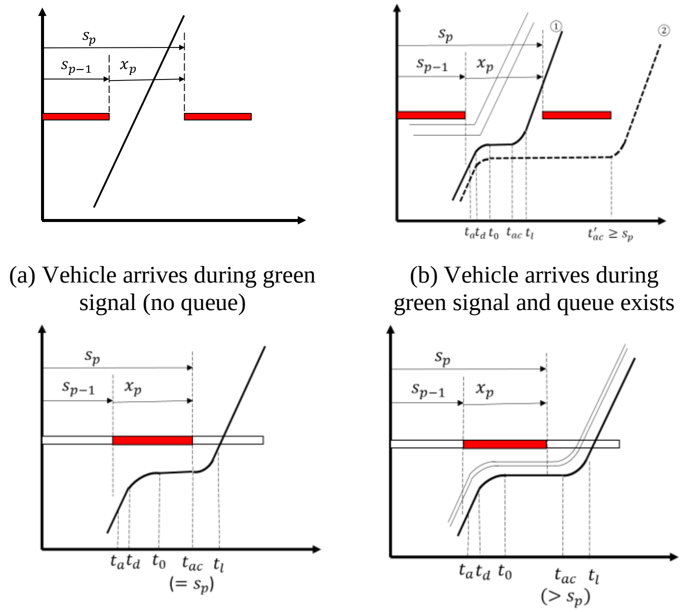

(a) Vehicle arrives during green signal (no queue)

(b) Vehicle arrives during green signal and queue exists

(c) Vehicle arrives during red signal (no queue)

(d) Vehicle arrives during red signal and queue exists

Figure 4 Vehicle average speed Approximation

B. End Stage Cost

The DP formulation so far does not impose any constraint on the cycle length. As shown in the next section, imposing such a constraint will invalidate the DP formulation. We propose two steps to address this issue: adding the end-stage cost to the DP formulation and a branch-and-bound method to refine the solution. First, in the last stage P, we modify the value function by adding the end stage cost f_e if the difference between the estimated cycle length C_e by DP and the predefined cycle length C is large. If σ denotes the tolerance, e.g., 5 seconds, and w denotes the weight, the revised value function for the last stage P can be expressed as:

$$V_p(s_p) = \min\{f_p(s_p, x_p) + V_{p-1}(s_{p-1}) + f_e | x_p \in X_p(s_p), p = P\} \quad (31)$$

The end-stage cost f_e can be expressed as in (32) while the estimated cycle length is the summation of the green time of all phases:

$$f_e = \begin{cases} 0, & if\ |C_e - C| \leq \sigma \\ w(C_e - C)^2, & otherwise \end{cases} \quad (32)$$

$$C_e = \sum_{p=1}^{P} x_p \quad (33)$$

The end-stage cost (32) with a proper weight works as a penalty function, ensuring that the obtained solution from the DP can result in a cycle length C_e close enough to the predefined cycle length C. To obtain a solution that can lead to C exactly, the second step applies a branch and bound method to refine the DP solution.

C. Branch and Bound Algorithm

To produce a signal timing solution that leads to exactly the predefined cycle length C, we need to add the following constraint to the decision variables in the DP formulation.

$$\sum_{p=1}^{8} x_p = C \quad (34)$$

This constraint however will invalidate the DP model as decisions cannot be made stage by stage when Eq. (34) is considered. In other words, DP cannot guarantee that the optimal phase durations sum up to a fixed cycle length. A branch and bound method is applied here to resolve the issue, which was used in the past to solve the Resources Constrained Shortest Path (RCSP) problem [40]. The method creates a tree by selecting one variable each time from an initial solution. Here the initial solution is produced by solving the DP formulation with the end-stage cost, as discussed above. The maximum level of the tree is the number of stages because the variable in a given set can only be used for branching once. Moreover, all branches at a given level of the tree have to be computed and analyzed before advancing to the next level. The numerical example of the branch and bound method will be provided in the net section. The can be summarized as below:

(1) DP with the end-stage cost is solved first to produce an initial solution.

(2) Define the error gain for stage/phase p:

$$EG_p(s_p, x_p) = f_p(s_p, x_p) \quad (35)$$

The error gain is the objective function in DP (total fuel consumption and travel time) for all vehicles traveling in stage p with stage variable s_p and decision variable x_p.

(3) If the estimated cycle length happens to be exactly the predefined cycle length C, the DP solution is an optimal solution. The algorithm stops.

(4) If the cycle length from the DP solution is *larger* than the predefined fixed cycle length (decision variable should be decreased), the selected phase for branching at each level is the one that has the *minimum* error gain. There could be multiple number of branching depending on the difference between the predefined cycle length and the cycle length from the DP solution. If the produced cycle length is *less* than the fixed cycle length (decision variable should be increased), the selected phase for branching would be the *maximum* error gain.

(5) The algorithm stops when the results of all branching (i.e., leaves) are feasible. The optimal solution is selected from the feasible solutions that satisfies the cycle length constraint while producing the minimum objective value.

IV. Numerical Experiments

We test the proposed CV-based signal timing optimization model and the DP method using data generated in VISSIM, which include the arrival time, arrival link (movement) and initial speed of each vehicle. The testing network contains a single intersection with a boundary of 300 meters upstream and downstream of the intersection to mimic the communication range of V2I. After comparing the approximated vehicle speed using our approximation method and the speed generated from VISSIM, we evaluate the proposed signal timing optimization method in three steps. First, we estimate the optimal cycle length using SYNCHRO, a widely used traffic signal design and optimization software tool, for different traffic demand cases. Next, for a given case, we apply different methods (see Table 2 and Table 3) to optimize the signal timing plans (phases and green splits), one for each method. We then evaluate the performance of each signal timing plan (i.e., each method) by applying the plan to the intersection and using IDM to generate vehicle trajectories, based on which to calculate the total cost. We also illustrate the procedure of the branch and bound algorithm and test the impact of the tolerance in the end-stage cost Eq. (32) on the performance of the proposed model. The values of all parameters used in this study can be found in the notation lists.

A. Speed approximation

In the proposed method, we approximate the vehicle speed as a function of the state variables and decision variables, as shown in Section III. Here we compare the vehicle speed between our method (Eq. (27)-(29)) and IDM simulation for the major streets in Figure 5. The suggested value of parameters in IDM are indicated in the notation lists. The platoon contains four vehicles. It is observed that the approximate speeds have the similar trend but not as smooth as the speed profile in IDM.

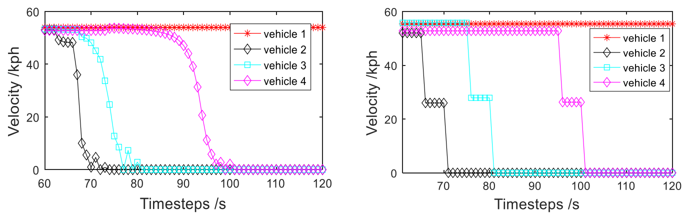

(a) IDM speed (b) Approximated speed

Figure 5 Speed Comparisons

In order to validate the speed approximation method is acceptable in fuel consumption estimation, the absolute differences of the fuel consumption with and without the speed approximation are estimated. It is observed that under all six cases, the mean absolute errors of fuel consumption using approximate speed are all less than 16%, which are considered acceptable in fuel consumption estimation.

B. Signal Timing Optimization

Different combinations of traffic demands and vehicle types are tested in order to evaluate the proposed signal optimization method. Vehicle arrivals at the boundaries of the intersection are generated from VISSIM. For each direction, 80% of the vehicles will go straight and the others will turn left. Six cases are tested to reveal the influence of traffic demands and vehicle types on the model performance. In Case I – III, vehicle demand is set to be 250 vph, 500 vph, and 800 vph, respectively. All vehicles are sedans (Type 5 in Table 1). In Case IV - VI, traffic demands are identical as in Case I - III, but the vehicle types are assigned differently. In the N-S directions, vehicles are assigned as Electric Vehicles (EVs, i.e., Vehicle type 1), while in the W-E directions, vehicles are assigned as buses (Vehicle type 7). Notice that generating all buses from one direction and all EVs from another is not very realistic. This is done here mainly to show more clearly the influences of the vehicle types on fuel consumption and signal timing.

We first test all models for 10 cycles. There are vehicles randomly generated to enter the network during the first 8 cycles, while during the last 2 cycles, there is no traffic demand. This guarantees the network is cleared by the end of the simulation. We test three signal control methods, as shown in Table 2 and Table 3. The first method is the actuated signal timing plan produced by SYNCHRO. The timing plan from SYNCHRO is then applied in IDM to update vehicle trajectories and estimate the objective function value, i.e., the total cost of fuel consumption and travel time using Eq. (1-5). The same procedure also applies to the other two models: the NOMAD solver in MATLAB and the DP method proposed here. The solver "NOMAD" uses a Mesh Adaptive Direct Search algorithm to solve non-differentiable and global nonlinear programs. It can solve non-convex MINLPs while it may not produce the global optimal solution. Since the starting point will directly influence the optimization results in NOMAD, we set the solution from SYNCHRO and DP respectively as the starting point in NOMAD to further reduce the cost. Dimensionality is another key factor affecting the performance of NOMAD. We test the model by updating the signal plan in various updating intervals (e.g., in every 1, 2, 5 or 10 cycles). The number of variables in NOMAD increases as the update frequency increases. For example, if we update the signal plan every cycle, there will be 80 variables in the total time span (10 cycles). The third model is the DP with the proposed end stage cost and the branch and bound method. DP update the signal plan every cycle. The results from DP without fixed cycle length constraints are also shown in the tables.

Table 2 and Table 3 summarize the results, in terms of the objective values, by different models for the six cases respectively, considering the influence of demand levels only (Table 2) and the combined demand levels and vehicle types (Table 3). The cycle lengths for different demand levels are determined by SYNCHRO: they are 60s for low traffic demand (250 vph), 65s for medium traffic demand (500 vph), and 85s for high demand (800vph), which are also the maximum value for the state variables in DP. Table 2 shows the cost from different models under various demand levels. NOMAD produces different solutions for different signal plan updating intervals and the starting points (from SYNCHRO in first four rows and from DP in the last row). We use the DP solution or the Synchro results as the initial points for NOMAD to make sure it can start with some reasonably good initial points. The best solutions from NOMAD are highlighted for each Case. Table 2 shows that if the signal plan is updated every cycle or every two cycles, the network performance are not improved since the total costs keep the same as its initial evaluation from the initial guess (SYNCHRO plan). However, a better solution may be obtained as the updating frequency decreases to every 5 or 10 cycles. This indicates that NOMAD has difficulties finding optimal solutions when the number of variables is relatively large. Table 2 also shows that different starting points in NOMAD can affect the optimal solutions. When compared with different models, DP outperforms SYNCHRO and achieves the same solution as NOMAD under low and medium demands in case I and case II. In case III, as the demand increases, DP results are still better than SYNCHRO but slightly worse than NOMAD. Table 3 shows the costs from different models under various demand levels and vehicle types. By comparing Case IV to Case I, we can see that the performance improvements of DP and NOMAD over SYNCHRO are more dramatic, which is also shown in Figure 6. Case IV incorporates buses in W-E direction, which produces much more fuel consumption than sedan in Case I. The cost generated from DP and NOMAD were both lower than SYNCHRO because SYNCHRO does not consider the influence of vehicle types on the fuel consumption when optimizing the signal timing. As the demand increases while still maintaining different vehicle types on NS and WE directions, the performance of DP is still better than SYNCHRO but slightly worse than NOMAD in medium (500vph) and high (800 vph) demand levels. Since NOMAD uses the optimal phase plan from SYNCHRO and DP as the starting point, it makes sense that the best NOMAD results are always better than or equal to SYNCHRO and DP for all cases. It is also observed that the results from DP without the fixed C constraint always have the lower objectives compared with the one with the fixed C constraint. This indicates that enforcing the fixed cycle length, i.e., for signal coordination purposes (and thus to the benefit of the entire system), may likely worsen the performance of individual intersections.

Table 2 Total Cost under Various Demand Levels

Model	Case I 250 vph, sedan	Case II 500 vph, sedan	Case III 800 vph, sedan	# of variables
1. SYNCHRO	49.64	162.39	368.99	/
2. NOMAD update every cycle	49.64	162.39	368.99	80
NOMAD update every 2 cycles	49.64	162.39	368.99	40
NOMAD update every 5 cycles	49.64	153.25	362.5	16
NOMAD update every 10 cycle	48.12	143.52	358.05	8
NOMAD update every 10 cycles & initial points from DP solution)	47.74	140.65	359.96	8
3. DP with fixed C constraint	47.74	140.65	360.73	/
(DP without fixed C constraint)	46.97	138.55	354.74	

Table 3 Total Cost under Various Demand Levels and Vehichle Types

Model	Case IV 250 vph; NS: Evs; WE: Bus	Case V 500 vph; NS: Evs; WE: Bus	Case VI 800 vph; NS: Evs; WE: Bus	# of variables
1. SYNCHRO	68.42	209.54	453.81	/
2. NOMAD update every cycle	68.42	209.54	453.81	80
NOMAD update every 2 cycles	68.42	209.54	453.81	40
NOMAD update every 5 cycles	68.42	168.29	453.81	16
NOMAD update every 10 cycle	65.78	180.67	434.37	8
NOMAD update every 10 cycles & initial points from DP solution)	63.37	169.54	436.65	8
3. DP with fixed C constraint	63.37	172.43	436.65	/
(DP without fixed C constraint)	61.25	163.54	433.36	

Figure 6 shows the performance improvements of NOMAD, DP with fixed cycle length, and DP without fixed cycle length over SYNCHRO. As shown in the dashed line, the model improvements of low and high demand levels are not as significant as the middle demand levels. This may be because under unsaturated but relatively heavy traffic conditions, there are more opportunities to optimize the splits and reduce the total cost of fuel consumption and travel time. Such opportunities tend to diminish when traffic is very light (all methods can work well) or very heavy (no method can work well). Furthermore, the performance improvements are more obvious if considering different vehicle types, as shown in Case IV – VI in Figure 6.

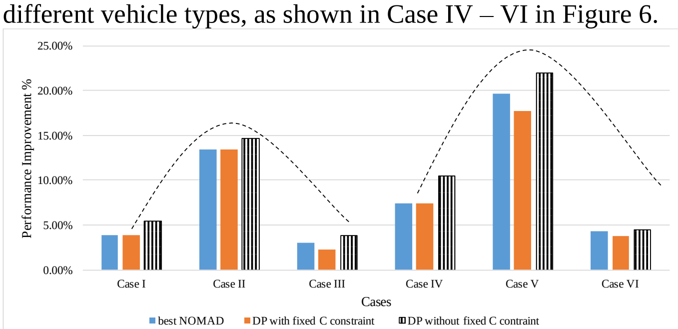

Figure 6 Improvement of Model Performance over SYNCHRO Results

Figure 7 shows the cost of fuel consumption and travel time separately for the four methods and six cases. For all cases, the cost of travel time is much larger than the cost of fuel consumption. Comparing cases IV, V, VI to cases I, II, III, it is observed that the influence of vehicle types is more significant on the cost of fuel consumption than travel time. Considering the same level of travel demand (e.g., case I and IV), the cost of fuel consumption is larger for the cases considering different vehicle types while the costs of travel time are similar.

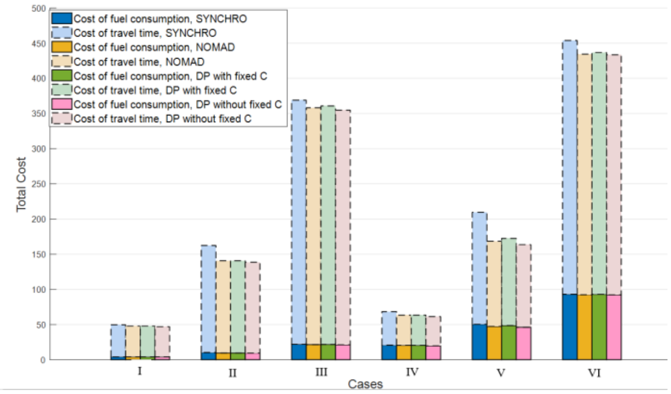

Figure 7 Total cost comparisons

The computation times for NOMAD and DP depend on the several factors, e.g., the update intervals of signal plans, whether considering vehicle types and traffic demands in the network. For NOMAD, the initial points and number of variables also influence the optimization time. Under high traffic demand, NOMAD can take up to 20 minutes to find a solution if signal timing is updated every 10 cycles; in some cases, NOMAD may fail to find any solution. For DP, the optimization time ranges from 10-20s per cycle (in the cycle-by-cycle signal optimization), depending on the traffic demand level. Currently the methods are implemented in Matlab and no code optimization is performed. When signal timing optimization is conducted in real time, the methods will be most likely programed in a more efficient language/platform (such as C or machine language) and the codes should be optimized to improve the performance. This can often significantly improve the computation time. Detailed investigation of this issue is beyond the scope of the paper, and may be pursued in future research.

In order to further verify the algorithm, the simulation period is extended from 10 cycles to 1 hour. For NOMAD, it cannot find a feasible solution even if the updating interval for signal timing is 10 cycles (larger updating intervals indicate fewer number of variables in NOMAD). Therefore we consider NOMAD fail to solve the signal optimization problem for the 1 hour simulation period and results are not shown here. In Table 4, the cost estimated from DP is less than SYNCHRO in every case. Case V has the largest improvement (10.02%) when considering various vehicle types under medium vehicle demands.

Table 4 Cost of Different models for 1 hour simulation

Model	Case I	Case II	Case III
	250 vph, sedan	500 vph, sedan	800 vph, sedan
1. SYNCHRO	277.72	685.39	1388.55
2.DP | Improvements (%)	266.39 | 4.08%	643.75 | 6.08%	1303.12 | 6.15%
Model	**Case IV**	**Case V**	**Case VI**
	250 vph; NS: Evs; WE: Bus	500 vph; NS: Evs; WE: Bus	800 vph; NS: Evs; WE: Bus
1. SYNCHRO	355.85	844.41	1658.3
2.DP | Improvements (%)	331.26 | 6.91%	759.81 | 10.02%	1623.86 | 2.08%

C. *Branch and Bound Algorithm*

This section illustrates how the branch and bound algorithm can be applied to the DP results (without the fixed cycle length constraint) to guarantee a solution with the fixed cycle length. Here we use the DP result of Case I in Table 2. Figure 8 shows the result from the DP by considering the end stage cost, which leads to a cycle length of 57s, 3 seconds lower than the predefined and fixed cycle length of 60s.

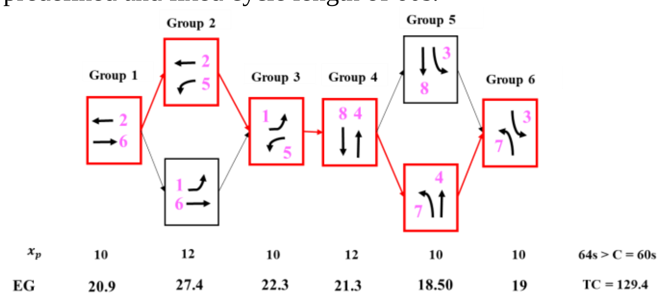

Figure 8 Estimated solution from DP

With the information of the DP solutions, the estimated Error Gain (EG) from DP, the total cost of fuel consumption and travel time, and the fixed cycle length, the branching can be selected based on the value of EG. In this case, since phase group 5 (phase 7) has the maximum EG, it is selected as the first level of branching, guided by the algorithm presented in the previous section. The nodes 1-3 enumerate each possible value of the decision variable for phase 7 in phase group 5, with the green time for phase 7 being 12, 13, 14, respectively. Only node 3 is feasible since its phase durations add up to the fixed cycle length 60s. For the node 1 – 2, the next level of branching is generated by the same rule. Figure 9 is the tree for branch and bound that lists all the feasible solutions with the total cost (TC) estimated using IDM. The feasible solution with the minimum objective value represents the optimal solution. It is observed that the total cost for the optimal solution in Figure 9 is larger than the total cost of the initial solution from DP (C=57s) because we sacrifice the signal performance by adding a fixed cycle length constraint using the branch and bound method.

The simulation results verify that the proposed DP with the two-step method is able to generate the phase durations that guarantee the given fixed cycle length and at the same time with objective to minimize the weighted traffic delay and fuel consumption. Ensuring the fixed cycle length makes it possible to extend the proposed model in the future to coordinate multiple intersections in a traffic corridor or network. Furthermore, the proposed method shows its advantages by considering the influence of vehicle types compared to the actuated traffic signal (i.e., SYNCHRO).

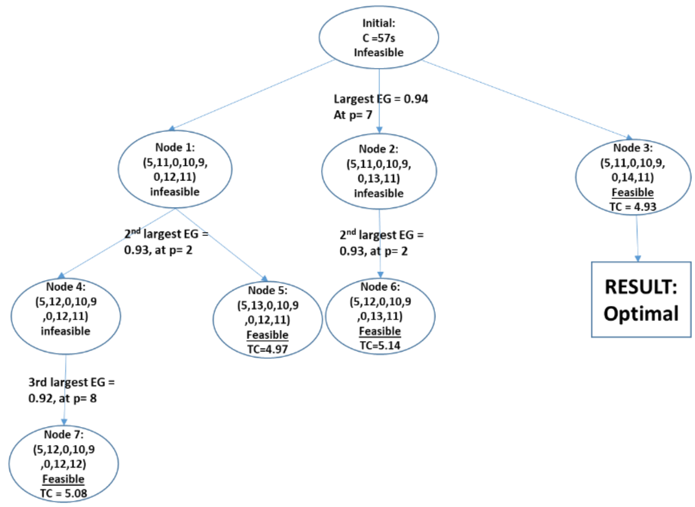

Figure 9 Branch and Bound Tree

D. *Tolerance parameter of branch and bound method*

In Eq.(32), we define a tolerance σ to calculate the end stage cost to find the DP solution. Different values of σ may produce difference intial solutions and influence the number of evaluations in the Branch and Bound algorithem. Here an evaluation means that for a given tentative signal timing plan, we need to estimate the objective in (25) using IDM, which may be time consuming. As shown in Figure 9, one node in the graph corresponds to one signal timing plan that needs to be evaluated. We test the tolerance σ from 0 to 10 and test the performance of the algorithm for Case I. In Figure 10, as σ increases, the total cost decreases slightly and attains its minimum value at $\sigma = 8$, but the number of evalutations increases dramatically. A very large value of σ (e.g., 10) will need to evalutate more timing plans, but may not help much to minimize the objective. Similar trends can be found for other cases. Seting $\sigma = 5$, as we use in this paper, seems a good balance between solution quality and the computational effort of the algorithm.

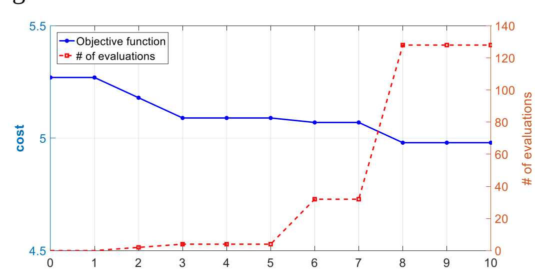

Figure 10 Influence of σ on the total cost for Case I

V. Conclusion

This paper presented a signal timing optimization model for a single intersection with a fixed cycle length under the CV environment. The algorithm utilized arrival information (speeds, locations, etc.) from CV as the input to optimize the green times by considering individual vehicles' fuel consumption and travel time. The problem was first formulated as a mixed-integer nonlinear program (MINLP) by applying the

IDM to predict vehicle trajectories. Such a formulation has a large dimension and a complex car-following model (the IDM). A DP formulation was then developed to approximate the MINLP. The overall problem was divided into stages (one stage for each signal phase). The objective is the summation of the objective of each stage. The objective function of a stage was approximated as a function of the state and decision variables of the stage only, by approximating the vehicle speeds and delays. We showed that imposing the fixed cycle length constraint would invalidate the DP formulation. We then applied a two-step method to address this issue. First, we added an end-stage cost to the DP formulation, defined by how much the DP solution violates the fixed cycle length constraint. This step forced the DP to produce a solution with a cycle length that is close to the given fixed cycle length. The second step was a branch and bound method to further refine the DP results to obtain a solution that produces the given cycle length exactly.

We evaluated the performance of the algorithm using data generated from traffic simulation. The results of the proposed DP model were compared with two other models. The first one is the traditional actuated signal timing plan generated by SYNCHRO. The second is to solve the MINLP formulation directly using the NOMAD solver in MATLAB. The results showed that the proposed DP method is always superior to SYNCHRO under all cases and can generate similar (slightly worse) solutions compared with NOMAD. However, NOMAD has difficulties finding optimal solutions when the number of variables is relatively large and the computational times of NOMAD are much larger than DP. This makes the proposed DP method more favorable when dealing with large scale problems.

Overall, the obtained solution by the proposed model ensures the (given) fixed cycle length, which is crucial for extending the proposed method to optimize and coordinate multiple traffic signals in a traffic corridor or network in the future. The objective for such corridor level optimization and coordination is to produce optimal offsets by minimizing the total fuel consumption and travel times of vehicles traveling along the coordinated movements [41]. For this, the proposed single-intersection optimization method, especially the DP reformulation and the two-step method, serves as a crucial component. The authors are investigating such a signal coordination problem and results may be reported in subsequent papers. Future research may also investigate how different penetration of CV-equipped vehicles will affect the performance of the proposed signal control method. This will require estimating the trajectories of vehicles that are not equipped with CV. When sample trajectory data from real world are available, certain stochastic models, e.g., Kalman filter based or Bayesian methods may be applied to estimate and predict the trajectories. For this, past work of the authors on estimating vehicle trajectories at signalized intersections may be helpful [42]. Recent study by Continental [43] can also be insightful for this. They applied the complete sensor set for an intersection to track vehicle trajectories, which can largely improve the penetration rate of CV. Furthermore, the proposed method needs to be tested using real world traffic signals and CV data. This will be pursued in future research.

Acknowledgment

The authors would like to thank the three anonymous referees for their insightful comments that helped improve the original version of the paper. The authors also thank Prof. Junmin Wang from the University of Texas at Austin for helpful discussions about the proposed model in this paper, and for the fuel consumption models his team developed in a joint research project with the authors. This research is partially supported by the C2SMART Tier 1 University Transportation Center (funded by USDOT) at the New York University via a grant to the University of Washington.

References

[1] EIA. (2016). How Much Gasoline Does the United States Consumed. U.S. Energy Information Administration.

[2] Schrank, D., Eisele, B., Lomax, T., & Bak, J. (2015). 2015 urban mobility scorecard. Texas Transportation Institute, August.

[3] Roess, R. P., Prassas, E. S., & McShane, W. R. (2011). Traffic engineering.

[4] Hoar, R., Penner, J., & Jacob, C. (2002). Evolutionary swarm traffic: if ant roads had traffic lights. In *Evolutionary Computation, 2002. CEC'02. Proceedings of the 2002 Congress on* (Vol. 2, pp. 1910-1915). IEEE.

[5] Datesh, J., Scherer, W. T., & Smith, B. L. (2011, June). Using k-means clustering to improve traffic signal efficacy in an IntelliDrive SM environment. In *Integrated and Sustainable Transportation System (FISTS), 2011 IEEE Forum on* (pp. 122-127). IEEE.

[6] Liu, H. X., & Di, X. (2010). Development of Algorithms for Travel Time-Based Traffic Signal Timing, Phase I–A Hybrid Extended Kalman Filtering Approach for Traffic Density Estimation along Signalized Arterials.

[7] Smith, B. L., Venkatanarayana, R., Park, H., Goodall, N., Datesh, J., & Skerrit, C. (2010). IntelliDriveSM Traffic Signal Control Algorithms. *University of Virginia*.

[8] Goodall, N. J. (2013). Traffic Signal Control with Connected Vehicles. A dissertation presented to the Faculty of the School of Engineering and Applied Sciences, University of Virginia. Retrieved from: http://people.virginia.edu/~njg2q/goodall_dissertation.pdf

[9] FHWA. Connected Vehicles. Retreived from: https://ops.fhwa.dot.gov/travelinfo/infostructure/aboutinfo.htm

[10] Goodall, N. J., Smith, B. L., & Park, B. B. (2013). Traffic signal control with connected vehicles. Transportation Research Record: Journal of the Transportation Research Board, 2381(1), 65-72.

[11] He, Q., Head, K. L., & Ding, J. (2012). PAMSCOD: Platoon-based arterial multi-modal signal control with online data. *Transportation Research Part C: Emerging Technologies*, *20*(1), 164-184.

[12] Lee, J., Park, B., & Yun, I. (2013). Cumulative travel-time responsive real-time intersection control algorithm in the connected vehicle environment. *Journal of Transportation Engineering*, *139*(10), 1020-1029.

[13] Sen, S., & Head, K. L. (1997). Controlled optimization of phases at an intersection. *Transportation science*, *31*(1), 5-17.

[14] Chen, S., Sun, D. J., Guan, S., & Guan, S. T. (2016). An Improved Adaptive Signal Control Method for Isolated Signalized Intersection. In *Transportation Research Board 95th Annual Meeting* (No. 16-6940).

[15] Feng, Y., Head, K. L., Khoshmagham, S., & Zamanipour, M. (2015). A real-time adaptive signal control in a connected vehicle environment. *Transportation Research Part C: Emerging Technologies*, *55*, 460-473.

[16] Zamanipour, M., Head, K. L., Feng, Y., & Khoshmagham, S. (2016). Efficient priority control model for multimodal traffic signals. *Transportation Research Record: Journal of the Transportation Research Board*, (2557), 86-99.

[17] Beak, B., Head, K. L., & Feng, Y. (2017). Adaptive Coordination Based on Connected Vehicle Technology. In the proceeding of Transportation Research Board 96th Annual Meeting, Washington DC. (No. 17-03523).

[18] Zhao, J., Li, W., Wang, J., & Ban, X. (2016). Dynamic Traffic Signal Timing Optimization Strategy Incorporating Various Vehicle Fuel

Consumption Characteristics. *IEEE Transactions on Vehicular Technology*, *65*(6), 3874-3887.

[19] Li, S. E., Hu, X., Li, K., & Ahn, C. (2014). Mechanism of vehicular periodic operation for optimal fuel economy in free-driving scenarios. *IET Intelligent Transport Systems*, *9*(3), 306-313.

[20] Xu, S., Li, S. E., Zhang, X., Cheng, B., & Peng, H. (2015). Fuel-optimal cruising strategy for road vehicles with step-gear mechanical transmission. *IEEE Transactions on Intelligent Transportation Systems*, *16*(6), 3496-3507.

[21] Li, S. E., Xu, S., Huang, X., Cheng, B., & Peng, H. (2015). Eco-departure of connected vehicles with V2X communication at signalized intersections. *IEEE Transactions on Vehicular Technology*, *64*(12), 5439-5449.

[22] Xu, S., Li, S. E., Cheng, B., & Li, K. (2017). Instantaneous feedback control for a fuel-prioritized vehicle cruising system on highways with a varying slope. *IEEE Transactions on Intelligent Transportation Systems*, *18*(5), 1210-1220.

[23] Dresner, K., & Stone, P. (2004). Multiagent traffic management: A reservation-based intersection control mechanism. In *Proceedings of the Third International Joint Conference on Autonomous Agents and Multiagent Systems-Volume 2* (pp. 530-537). IEEE Computer Society.

[24] Dresner, K., & Stone, P. (2005,). Multiagent traffic management: An improved intersection control mechanism. In *Proceedings of the fourth international joint conference on Autonomous agents and multiagent systems*(pp. 471-477). ACM.

[25] Au, T. C., Zhang, S., & Stone, P. (2014). Semi-autonomous intersection management. In *Proceedings of the 2014 international conference on Autonomous agents and multi-agent systems* (pp. 1451-1452). International Foundation for Autonomous Agents and Multiagent Systems.

[26] Li, Z., Chitturi, M. V., Zheng, D., Bill, A. R., & Noyce, D. A. (2013). Next-generation intersection control algorithm for autonomous vehicles. In *Transportation Research Board 92nd Annual Meeting* (No. 13-2185).

[27] Li, L., & Wang, F. Y. (2006). Cooperative driving at blind crossings using intervehicle communication. *IEEE Transactions on Vehicular Technology*, *55*(6), 1712-1724.

[28] Li, L., Wen, D., & Yao, D. (2014). A survey of traffic control with vehicular communications. *IEEE Transactions on Intelligent Transportation Systems*, *15*(1), 425-432.

[29] Xu, B., Ban, X. J., Bian, Y., Li, W., Wang, J., Li, S. E., & Li, K. (2018). Cooperative Method of Traffic Signal Optimization and Speed Control of Connected Vehicles at Isolated Intersections. IEEE Transactions on Intelligent Transportation Systems, (99).

[30] Han, K., & Gayah, V. V. (2015). Continuum signalized junction model for dynamic traffic networks: Offset, spillback, and multiple signal phases. Transportation Research Part B: Methodological, 77, 213-239.

[31] He, Q., Head, K. L., & Ding, J. (2014). Multi-modal traffic signal control with priority, signal actuation and coordination. *Transportation research part C: emerging technologies*, 46, 65-82.

[32] Feng, Y., Zamanipour, M., Head, K. L., & Khoshmagham, S. (2016). Connected Vehicle–Based Adaptive Signal Control and Applications. *Transportation Research Record: Journal of the Transportation Research Board*, (2558), 11-19.

[33] Koonce, P. (2008). *Traffic signal timing manual* (No. FHWA-HOP-08-024). United States. Federal Highway Administration.

[34] Li, W., & Ban, X. J. (2017). Traffic signal timing optimization in connected vehicles environment. In Intelligent Vehicles Symposium (IV), 2017 IEEE (pp. 1330-1335). IEEE.

[35] USDOT. Traffic Control Systems Handbook: Chapter 7. Local Controllers. Retrieve from: http://ops.fhwa.dot.gov/publications/fhwahop06006/chapter_7.htm

[36] Smith, J. C., & Taskin, Z. C. (2008). A tutorial guide to mixed-integer programming models and solution techniques. Optimization in Medicine and Biology, 521-548.

[37] Treiber, M., Hennecke, A., & Helbing, D. (2000). Congested traffic states in empirical observations and microscopic simulations. *Physical review E*, *62*(2), 1805.

[38] Talebpour, A., & Mahmassani, H. S. (2014). Modeling acceleration behavior in a connected environment. Celebrating 50 Years of Traffic Flow Theory, 87.

[39] Khondaker, B., & Kattan, L. (2015). Variable speed limit: A microscopic analysis in a connected vehicle environment. *Transportation Research Part C: Emerging Technologies*, *58*, 146-159.

[40] Danczyk, A., & Liu, H. X. (2011). A mixed-integer linear program for optimizing sensor locations along freeway corridors. *Transportation Research Part B: Methodological*, *45*(1), 208-217.

[41] Li, W., Ban, X. J., & Wang, J. (2016). Traffic signal timing optimization incorporating individual vehicle fuel consumption characteristics under connected vehicles environment. In *Connected Vehicles and Expo (ICCVE), 2016 International Conference* on (pp. 13-18). IEEE.

[42] Sun, Z., and Ban, X., 2013. Vehicle trajectory reconstruction for signalized intersections using mobile traffic sensors. *Transportation Research Part C* 36, 268-283.

[43] Continental AG. (2018). New Avenues: Vehicle Technology and Specifically Connectivity Can Ease Smart City Traffic. Retrieved from: https://www.continental-corporation.com/en-sg/press-/press-releases/ces-press-conference-118624.

Wan Li received her B.S. degree in traffic engineering from Sun Yat-Sen University, Guangzhou, China, in 2012 and her M.S. degree in civil engineering from Louisiana State University, Baton Rouge, LA, USA, in 2014. She is currently working toward her Ph.D. degree in civil engineering from the University of Washington, Seattle, WA, USA. Her current research interests include traffic signal optimization with connected/automated vehicles and transportation big data analytics.

Xuegang (Jeff) Ban is an Associate Professor with the Department of Civil and Environmental Engineering at the University of Washington. He received his B.S. and M.S. in Automotive Engineering from Tsinghua University, and his M.S. in Computer Sciences and Ph.D. in Transportation Engineering from the University of Wisconsin at Madison. His research interests are in Transportation Network System Modeling and Simulation, Urban Traffic Modeling and Control, and Intelligent Transportation Systems (ITS). His recent research focuses on applying system analysis/control tools and data analytics methods to understand the impact of emerging technologies (such as connected/automated vehicles (CAVs) and shared mobility) to transportation network systems, including traffic signal optimization and control under the CAV environment. He has published over 120 papers in refereed journals and conference proceedings. He is an Editor / Associate Editor of *IEEE Transactions on Intelligent Transportation Systems*, *Transportation Research Part C*, and *Journal of Intelligent Transportation Systems*, and serves on the editorial board of *Transportation Research, Part B*, *Networks and Spatial Economics*, and *Transportmetrica B*. He is a member of the Network Modeling Committee (ADB30) and a member of the Vehicle-Highway Automation Committee (AHB30) of the Transportation Research Board (TRB).